ISSN 1027-5495. Functional Materials, 22, No.2 (2015), p. 199-206.
doi:http://dx.doi.org/10.15407/fm22.02.199

In vitro study of NCs/dyes complexes accumulation and dyes release kinetics in rat hepatocytes

S.L.Yefimova, T.N.Tkacheva, N.S.Kavok, V.K.Klochkov, A.V.Sorokin

Institute for Scintillation Materials, STC "Institute for Single Crystals",
National Academy of Sciences of Ukraine,
60 Lenin Ave., 61001 Kharkiv, Ukraine

Received February 15, 2015

Using fluorescence microspectoscopy and FRET-labeling of various nano-scale carriers (NCs) the efficiency and kinetics of NCs/dye molecules complexes accumulation in living cells and dye release have been studied. Organic liposome vesicles and inorganic nanoparticles (CeO_2 and $GdYVO_4:Eu^{3+}$) were used as NCs. NCs/dyes complexes formed in aqueous solutions have been characterized. It has been shown that NCs based on $GdYVO_4:Eu^{3+}$ nanoparticles exhibit the most effective accumulation in cells and provide very fast release of the lipophilic cargo (dyes molecules). Lipophilic compound (cholesterol) embedded into the NCs/dyes complexes decreases noticeably the rate of lipophilic dyes release and reduces the affinity of the complex interaction with hepatocytes. $GdYVO_4:Eu^{3+}$ NPs could be used as a nano-scale platform for controlled intracellular delivering of hydrophobic agents.

Keywords: nano-scale carriers, Forster Resonance Energy Transfer, dye release, cholesterol, living cells.

Используя метод флуоресцентной микроспектроскопии и FRET-мечение разных типов наноконтейнеров (НК) изучена эффективность и кинетика аккумуляции комплексов НК/молекулы красителей, а также кинетика высвобождения красителей в живые клетки. В качестве НК использовали органические липосомальные везикулы и неорганические наночастицы (CeO2 и GdYVO4:Eu3+). Охарактеризованы комплексы НК/красители, полученные в водных растворах. Показано, что НК на основе GdYVO4:Eu3+ наночастиц (НЧ) обеспечивают наиболее эффективную аккумуляцию в клетках и очень быстрое высвобождение липофильного содержимого (молекул красителей). Однако добавление в систему дополнительного липофильного компонента (холестерина) приводит к уменьшению скорости высвобождения красителей и к снижению эффективности взаимодействия комплексов с гепатоцитами. Показано, что НЧ GdYVO4:Eu3+ могут быть использованы в качестве наноразмерной платформы для контролируемой внутриклеточной доставки гидрофобных соединений.

Вивчення акумуляції комплексів НК/барвники і кінетики вилучення барвників у клітинах гепатоцитів щурів в експериментах *in vitro*. *С.Л.Єфімова, Т.М.Ткачова, Н.С.Кавок, В.К.Клочков, А.В.Сорокін*.

Використовуючи метод флуоресцентної мікроспектроскопії і FRET-міченння різних типів наноконтейнерів (НК) вивчено ефективність і кінетику акумуляції комплексів НК/молекули барвників, а також кінетику вилучення барвників у живі клітини. В якості НК використано органічні ліпосомальні везикули і неорганічні наночастинки (CeO2 і GdYVO4:Eu3+). Охарактеризовано комплекси НК/барвники, що отримані у водних розчинах. Показано, що НК на основі GdYVO4:Eu3+ наночастинок (НЧ) забезпечують найбільш ефективну акумуляцію у клітинах і дуже швидке вилучення ліпофільного вантажу (молекул барвників). Проте додавання у комплекс додаткового ліпофільного компонента (холестерину) призводить до зменшення швидкості вилучення барвників і зниження ефективності взаємодії комплексів з гепатоцитами. Виявлено, що НЧ GdYVO4:Eu3+ можуть бути використані в якості нанорозмірної платформи для контрольованої внутрішньоклітинної доставки гідрофобних сполук.

1. Introduction

Nanotechnology is a modern technology that deals with nano-mater size objects on several levels: materials, devices and systems [1]. One of the most research area of nanotechnology is nanomedicine, tissue- and cell-specific drug delivery in particular [1–8]. Nanomedicine focuses on formulation of therapeutic agents in biocompatible nanocarriers (NCs), such as lipid vesicles, micellar systems, nanocapsules, dendrimers, biopolymers and inorganic nanoparticles (NPs). These nano-scale carriers improve the solubility of poorly water-soluble drugs, prolong the half-life of drug systemic circulation, and can provide controlled drug release [3–8]. In the last two decades, a number of nanocarrier-based therapeutic and diagnostic agents have been developed for the treatment of cancer, diabetes, pain, asthma, allergy, infections, and so on [3–8]. Moreover, one of the major advantages that nanotechnology offers is targeted drug delivery to the site of disease either through passive or active targeting of drugs to the site of disease to minimize systemic side effect and lower therapeutic toxicity [3, 6].

Despite the rather wide applications of inorganic NPs as therapeutic, diagnostic and imaging agents, their application as a nano-scale platform for nanodrug development is still under study [3–5, 9, 10]. In recent years some NPs, i.e. nanocrystalline ceria and rare-earth doped orthovanadate NPs have revealed high biological activity (oxidative stress prevention, anti-inflammation and neuroprotective activity, antitumor effect) that attracts a lot of interest to these objects as a platform for design of multi-functional drug with the synergetic effect [11–14]. Furthermore, the particle surface can be seen as a platform where multiple functionalization and targeting groups can be easily grafted [7, 10]. It was shown that NPs interact with organic molecules via electrostatic and van-der-Waals forces that leads to the adsorption of organic molecules on the NPs surface and formation hybrid complexes NPs/organic molecules, where the latter could be arranged in the form of ordered aggregates [13, 15]. Despite the attractive prospects of NPs application as an emerging nanoplatform for drug delivery, pathways and dynamics of NPs entering into cells and kinetics of active compound release from such hybrid complexes should be considered to archive high delivery efficiency and controlled drug release.

In the present paper, we report *in vitro* study of the efficiency and dynamics of various NCs/dye molecules complexes accumulation in living cells and dye release kinetics using fluorescence microspectroscopic techniques. As NCs we use organic liposome vesicles and inorganic NPs (CeO_2 and $GdYVO_4:Eu^{3+}$). The dyes used as mimic hydrophobic drug molecules. To study the dye release in dynamics, we use a pair of dyes, so-called FRET-pair (Forster Resonance Energy Transfer [16]), DiO and DiI dye molecules, encapsulated in or adsorbed on NCs and λ-ratiometry method of fluorescence detection based on fluorescence recording at two wavelengths [17–19].

2. Materials and methods

2.1. Chemicals

Fluorescent hydrophobic dyes 3,3′-dioctadecyloxacarbocyanine perchlorate (DiO), 1,1′-dioctadecyl-3,3,3′,3′-tetramethylindocarbocyanine perchlorate (DiI), L-a-phosphatidylcholine (PC) from egg yolk were purchased from Sigma-Aldrich (USA) and used without purification. Chloroform (Sigma-Aldrich) used to prepare lipid and dye stock solutions was a spectroscopic grade product. Isopropyl alcohol (Sigma-Aldrich) was also of spectroscopic grade. EDTA, HEPES buffered saline solution (HBSS), Bovine Serum Albumin (BSA) and Eagle's medium for cell treatment were purchased from Sigma-Aldrich. To prepare aqueous solutions of the dyes with NCs, double distilled water was used.

2.2. NPs synthesis

The aqueous colloidal solutions of $GdYVO_4:Eu^{3+}$ and CeO_2 have been synthesized according to the method reported earlier [13]. NPs were characterized using Transmission Electron Microscopy (TEM-125K electron microscope, Selmi, Ukraine) and Dynamic Light Scattering method (Zeta-PALS analyzer, Brookhaven Instruments Corp., USA).

2.3. Preparation of lipid vesicles with DiO and DiI dyes

Unilamellar PC lipid vesicles containing DiO and DiI dyes were prepared by the extrusion method [20]. Briefly, appropriate amount of PC (40 mg/ml) and dyes (10^{-3} M) stock solutions in chloroform were mixed in a flask and dried until complete chloroform evaporation using a rotary evaporator (Rotavapor R-3, Buchi). The thin lipid-dyes film was then hydrated with 2 ml of double distilled water. Final concentration of PC

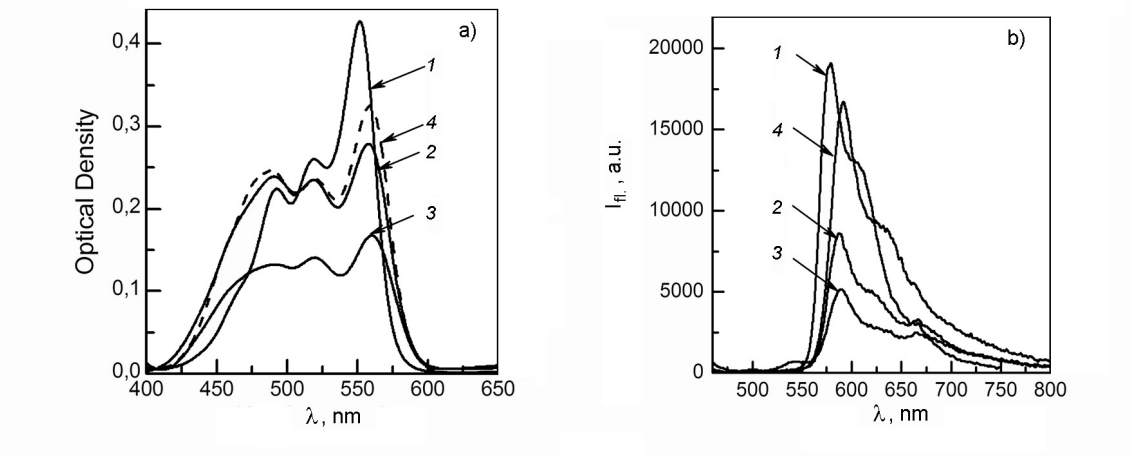

Fig. 1. Absorption (a) and fluorescence (b) spectra of the complexes: *1* — PC liposomes/dyes; *2* — $GdYVO_4:Eu^{3+}$/dyes; *3* — CeO_2/dyes; *4* — $GdYVO_4:Eu^{3+}$/dyes/cholesterol complexes. λ_{exc} = 440 nm.

was $1 \cdot 10^{-3}$ M. The obtained lipid-dyes suspension was finally extruded through 100 nm pore size polycarbonate filter using a mini-extruder (Avanti Polar Lipids, Inc., USA). The concentrations of each dye in liposomal suspension were $2 \cdot 10^{-5}$ M.

2.4. Preparation of NPs/dyes complexes

5 ml of water colloidal solutions of $GdYVO_4:Eu^{3+}$ or CeO_2 (0.83 g/l) NPs and 5 ml of DiO and DiI dyes ($3.3 \cdot 10^{-5}$ M) solutions in isopropyl alcohol were mixed in a flask using a magnetic stirrer and then 10 ml of double distilled water was added. The mixture was carefully stirred using a rotary evaporator during 1 h to a complete evaporation of isopropyl alcohol. Final concentration of each dye was $2 \cdot 10^{-5}$ M, concentration of $GdYVO_4:Eu^{3+}$ and CeO_2 NPs was 0.5 g/l.

In complexes containing cholesterol, it solution in isopropyl alcohol (0.1 M) was added at the stage of mixture preparation. Final concentration of cholesterol was 0.25 g/l.

2.5. Cell labeling procedure

Isolated rat hepatocytes from male Wistar rats were obtained by the method described by Wang after dissociation of the liver with 2 mM EDTA [21]. Cell viability was assessed via the trypan blue exclusion test. The cell viability 95 % and yield $1.5 \cdot 10^7$ cells$\cdot g^{-1}$ liver is in good agreement with those of previously described [21]. To study the efficiency of NCs accumulation in hepatocytes, cells pellet (50 μl 10^7 cells/ml) were incubated with suspension of NCs/dyes complexes (50 μl) in 1 ml of Eagle's medium with 10 % fetal calf serum at 37°C for required time intervals. After each time interval, non-bound NCs were removed by centrifugation at 500 g and washing-out by adding HBSS buffer (pH 7.4) with 0.1 % BSA and cell fluorescence images were analyzed used fluorescence microscopy.

To study the kinetics of dye release from NCs of different types to hepatocytes, cells pellet (50 μl 10^7 cells/ml) were incubated with suspension of NCs/dyes complexes (450 μl) at the room temperature for 15 minutes. Afterwards non-bound liposomes or NCs were removed by centrifugation at 500 g and washing-out by adding HBSS buffer (pH 7.4) with 0.1 % BSA. Then 500 μl of HBSS buffer with 0.1 % BSA were added to all complexes and incubated at 37°C for required time intervals. Then cell images were analyzed used fluorescent microspectroscopy.

2.6. Cell imaging, spectroscopy and microspectroscopy

Fluorescence spectra of the solutions were taken with a spectrofluorimeter Lumina (Thermo Scientific, USA). Cell visualization was carried out using fluorescent microscope Olympus IX 71 supplied with digital camera Olympus C-5060 with the magnification of ×1000 in the conditions of oil immersion. Fluorescence was excited by a xenon lamp 75 W using BP 460-490 nm filters. Microspectroscopy at the area of interest was carried out using spectral detector USB 4000 (Ocean Optics) connected with Olympus IX71.

The total brightness of the cell images obtained at different time intervals was estimated using image bitmap analysis (Adobe Photoshop CS3 software package).

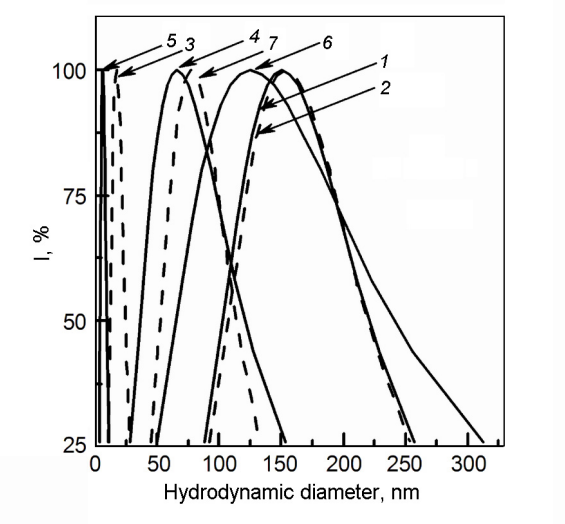

Fig. 2. Hydrodymanic diameters: *1* — PC liposomes; *2* — PC liposomes/dyes complexes; *3* — $GdYVO_4:Eu^{3+}$ NPs; *4* — $GdYVO_4:Eu^{3+}$/dyes complexes; *5* — CeO_2 NPs; *6* — CeO_2/dyes complexes; *7* — $GdYVO_4:Eu^{3+}$/dyes/cholesterol complexes.

3. Results and discussions

3.1. *NCs/dyes complexes characterization*

DiO and DiI dyes are well-known fluorescent lipophilic tracers and FRET pair as well [22–25]. The dyes are weakly fluorescent in water (due to aggregation), while highly fluorescent and quite photostable when incorporated into cell membrane exhibiting green and orange fluorescence (emission maxima 505 and 575 nm), respectively [22–25]. Being incorporated in lipid bilayers of PC liposomes, the dyes show no aggregation, whereas monomer absorption with main maxima centered at 492 nm (DiO) and 552 nm (DiI) and shoulders centered at 462 nm and 519 nm, respectively (Fig. 1a, curve *1*). The main maxima are assigned to the 0→0 vibronic transition between the electronic molecular ground state and the first excited one in the dye molecules, whereas the shoulders, to the 0→1 vibrational excitation of the ground to the first excited state, respectively that is typical for polymethine dyes [26]. Loading of PC liposomes with cationic polymethine dyes does not provoke remarkable changes in the liposome hydrodynamic diameter (Fig. 2, curves *1* and *2*). The dyes DiO and DiI possess long hydrocarbon tails $C_{18}H_{37}$ and in lipid bilayers of PC liposomes the dyes locate in such a way that their charged chromosphere groups are in contact with water, whereas long tails are embedded into the lipid bilayer (Fig. 3a). Enhanced concentration of the DiO and DiI dyes in the lipid bilayers of PC liposomes ensures the necessary distance between the donor DiO and acceptor DiI molecules for efficient FRET between them at the excitation within the donor absorption band that is confirmed by the fluorescence spectrum (Fig. 1b, curve *1*). As shows Fig. 1b, at the excitation at 440 nm, the efficiency of FRET is about 100 %, the donor DiO fluorescence with $\lambda_{max} = 505$ nm is not observed.

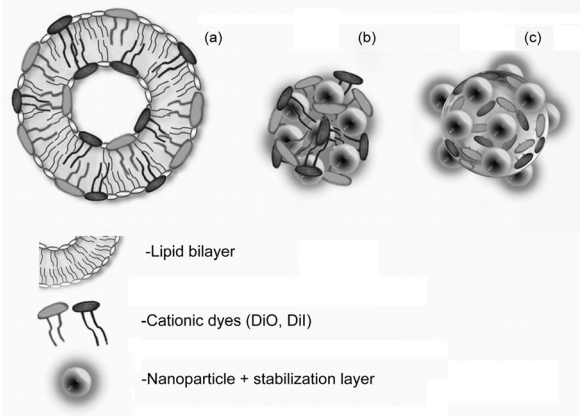

Fig. 3. Schematic representation of the PC liposomes/dyes (a) NPs/dyes (b) and NPs/dyes/cholesterol complexes (c).

In water solutions $GdYVO_4:Eu^{3+}$ and CeO_2 nanoparticles are stabilized by sodium citrate that imparts a negative charge to a particle surface [13]. Cationic dyes molecules are attracted by the NPs surface due to Coulomb interaction. That provokes a close packing of dye molecules near the charged surface, an increase of the dyes local concentration followed by the dyes partial aggregation (Fig. 1a, curves *2* and *3*). Furthermore, the NPs/dyes assemblies coalesce to form larger complexes due to the surface charge neutralization and hydrophobic interactions between the dye molecules (Fig. 3b) [13]. This statement is confirmed by the DLS data, which clearly show a sharp increase in NPs hydrodynamic diameters in solutions with the dyes from 17 nm up to 66 nm for $GdYVO_4:Eu^{3+}$ NPs and from 7 nm up to 125 nm for CeO_2 NPs, Fig. 2. The dye concentration near the NPs surface in formed complexes causes very effective FRET between DiO and DiI dyes (Fig. 1b, curves *2* and *3*).

In NPs/dyes/cholesterol complexes, the hydrophobic DiO and DiI dyes are concentrated in nano-sized cholesterol drops, which are stabilized by the $GdYVO_4:Eu^{3+}$

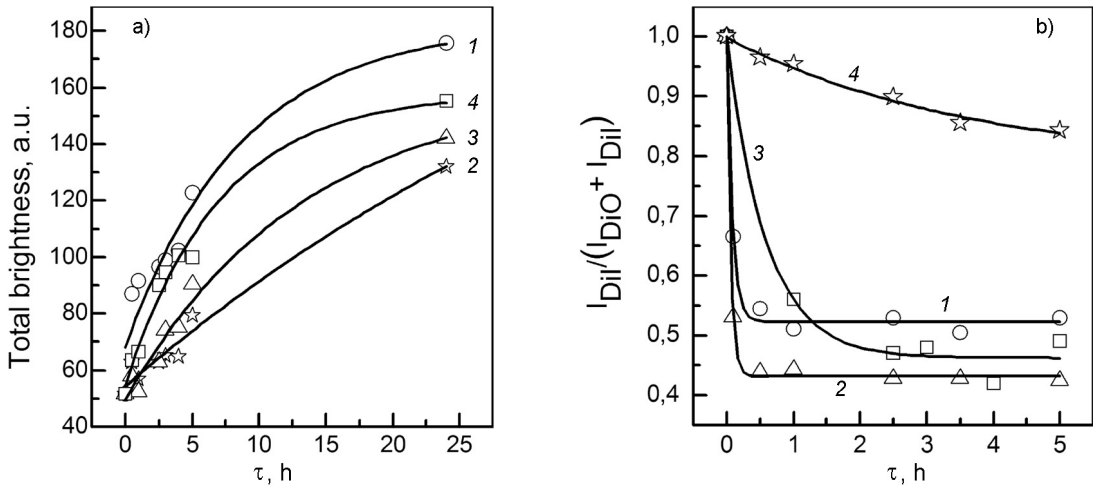

Fig. 4. (a) Total brightness changes in time for rat hepatocytes incubated with different nano-scale carriers: *1* — $GdYVO_4:Eu^{3+}$/dyes; *2* — $GdYVO_4:Eu^{3+}$/dyes/cholesterol; *3* — CeO_2/dyes; *4* — PC liposomes/dyes complexes. Straight lines are fitting of the experimental data with $B = B_0 \cdot e^{t/\tau_{sat}}$ law; (b) Time traces of FRET ratio $I_{DiI}/(I_{DiO} + I_{DiI})$ in red hepatocytes: *1* —$GdYVO_4:Eu^{3+}$/dyes; *2* — PC liposomes/dyes; *3* — CeO_2/dyes; *4* — $GdYVO_4:Eu^{3+}$/dyes/cholesterol complexes. Straight lines are fitting of the experimental data with Eq. (1).

NPs as shown schematically in Fig. 3c. The concentration of the dyes molecules in cholesterol conformed by the bathochromic shift of the absorption and fluorescence spectra (Figs. 1a and b). The NPs/dyes/cholesterol complexes are of about 70 nm in diameters (Fig. 2, curve *7*).

At used ratios of NCs/dyes molecules, all NCs/dyes complexes are stable at least two weeks without any changes in their aggregation and optical properties.

3.2. Interaction of NCs/dyes complexes with rat hepatocytes

One of the features of hepatocytes is their high functional-metabolic activity even in the isolated state that makes them attractive to study metabolic processes at the cellular level. In our research, we analyze (i) the dynamic and efficiency of NCs/dyes complex accumulation in the cells and (ii) kinetics of the dyes release from the NCs to the cells. To study the efficiency of NCs/dyes uptake by the hepatocytes, the increase in total brightness of the cell images taken in different time intervals of cells incubation with the NCs/dyes complexes was analyzed. The more complexes containing fluorescent dyes are uptaken by the cells, the brighter cell image should be. To take into account intact NCs/dyes complexes fluorescence, where FRET emission is dominate, and the complexes where dye leakage is observed and, consequently, the donor fluorescence part is remarkable, we analyze total image brightness in both green and red channels.

Fig. 4a shows different efficiency of NCs/dyes complexes accumulation depending on NCs type. It is known that kinetics, amount and mechanism of NPs uptake by cells depends strongly on numerous factors such as NPs type, size and surface properties, incubation conditions, cell type, etc. [27–29]. Analyzing the efficiency of NCs/dyes complexes accumulation, we should take into account the affinity of NCs interaction with the cell membrane. It is known that neutral and negatively charged NPs adsorbed much less on the negatively charged cell-membrane surface and consequently show lower level of internalization as compared to the positively charged particles [27–29]. As seen in Fig. 4a, $GdYVO_4:Eu^{3+}$ NPs/dyes complexes reveal the most effective accumulation in rat hepatocytes. After 24 h incubation the brightness of the cells incubated with $GdYVO_4:Eu^{3+}$ NPs/dyes complexes was the highest. At the same time, the characteristic time of the cell saturation with $GdYVO_4:Eu^{3+}$ NPs/dyes complexes (τ_{sat}) estimated using the exponential law of brightness change (B) as a function of an incubation time (t) $B = B_0 \cdot e^{t/\tau_{sat}}$, is about 9 h (Fig. 4a, curve *1*). The observed effect correlates with the data presented in [27–29]. We suppose that the cationic dye adsorption on the surface of NPs leads to the partial neu-

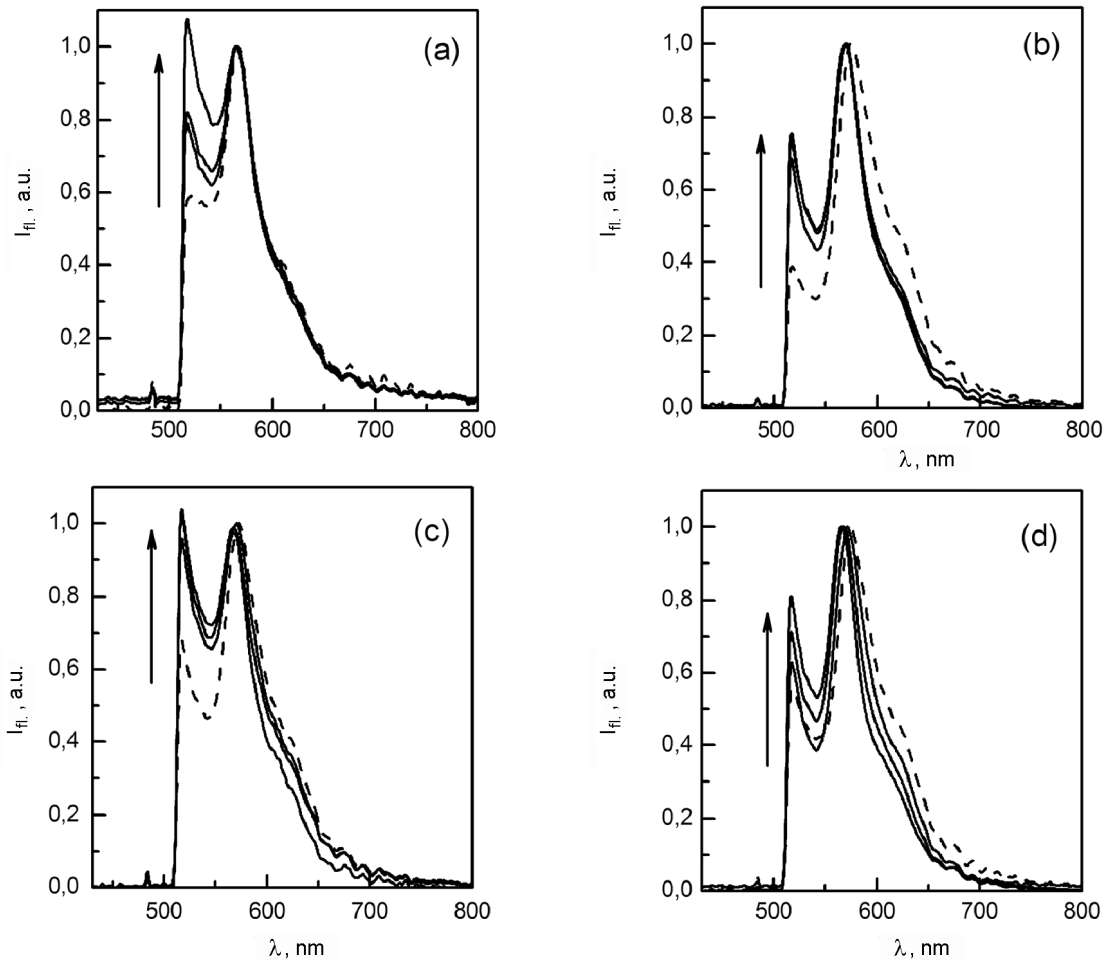

Fig. 5. Fluorescence spectra of the complexes taken from different times of cell incubation (0, 1, 3 and 5 hours) with PC liposomes/dyes (a), $GdYVO_4:Eu^{3+}$/dyes (b), CeO_2/dyes (c) and $GdYVO_4:Eu^{3+}$/dyes/cholesterol (d) complexes. Excitation with BP 460–490 filter.

tralization of NPs negative charge, while formation of large NPs/dyes complexes provokes a creation of local regions with a positive charge that facilitates the adsorption of complexes on a cell membrane (Fig. 3b).

On the contrary, NPs/dyes/cholesterol complexes, where dyes are concentrated in nano-sized cholesterol drops stabilized by the $GdYVO_4:Eu^{3+}$ NPs, show the lowest affinity of interaction with the cells (Fig. 4a, curve *2*). That could be explained by the stabilization of the cholesterol/dyes drops with negatively charged NPs (Fig. 3c). Moreover, cholesterol internalization by the cells is known to require specific receptor-mediated pathway [30] that can affect the kinetics of this process. Obtained τ_{sat} value (50 h) for $GdYVO_4:Eu^{3+}$ NPs/dyes/cholesterol complex is about 6 times higher as compared to the $GdYVO_4:Eu^{3+}$ NPs/dyes ones.

NPs/dyes complexes on the base of CeO_2 NPs show lower efficiency of their interaction with the cells as compared to $GdYVO_4:Eu^{3+}$ NPs/dyes complexes. After 24 h incubation, the total brightness of the cells is much smaller, the saturation time is larger (τ_{sat} = 13 h), Fig. 4a, curve *3*. We ascribe observed features to the larger size of CeO_2 NPs/dyes complexes (Fig. 2) that probably requires another mechanism of internalization, e.g. clathrin-mediated endocytosis [27].

PC liposomes as NCs have large affinity to cell membranes interaction facilitated by the positively charged dye fluorophores incorporated in lipid bilayers (Fig. 4a, curve *4*). The cell total brightness after 24 h incubation is a bit smaller than that for $GdYVO_4:Eu^{3+}$ NPs/dyes complexes, while kinetics of PC liposomes/dyes interaction exhibit a pattern similar to $GdYVO_4:Eu^{3+}$ NPs/dyes complexes (τ_{sat} = 7 h).

Kinetic parameters of the dye release from NCs to the cells that effect the redis-

tribution of the donor/acceptor fluorescent signal also should be taken into consideration. Below we will show that obtained data correlate with the efficiency of complexes accumulation discussed above.

To study the kinetics of the hydrophobic dyes release from the NCs to cells (cell membranes and intracellular space), we analyze changes in time of the FRET ratio $I_{DiI}/(I_{DiO} + I_{DiI})$, where I_{DiI} and I_{DiO} are fluorescence intensities measured at the acceptor DiI and donor DiO maxima, respectively [17–19]. When dyes molecules release from NCs and diffuse apart in the cell membrane or inside of cells depending on mechanisms of NCs-to-cell interaction, the distance between donors and acceptors will increase eliminating the energy transfer and a redistribution of the donor and acceptor peak intensities will be observed [16–19]. For all complexes under study, the remarkable decrease in the FRET ratio was observed in time, which is accompanied by the blue shift of fluorescence maxima (Fig. 5). That indicates dyes release from NCs and transition to other environment, most probably, to cell membrane.

The process of redistribution of the dyes between NCs and the cells can be described by first-order reaction kinetics in the following form [25, 31]:

$$\left(\frac{I_{DiI}}{(I_{DiO} + I_{DiI})}\right)_{(t)} = \left(\frac{I_{DiI}}{(I_{DiO} + I_{DiI})}\right)_{(0)} e^{-Kt}, \quad (1)$$

where K is the dye release rate constant (the dye leakage coefficient).

The FRET ratio changes are presented in Fig. 4b. A nonlinear fit (Eq. 1) of the FRET ratio changes was generated by the method of last-squares and allows K values for all NCs/dyes complexes to be obtained (Table).

For first-order reactions one can also use the dye release half-life (in our case, time for the initial FRET ratio to be reduced by 1/2), which can be obtained as [25]:

$$\tau_{1/2} = \frac{\ln 2}{K}. \quad (2)$$

As show Table and Fig. 4b, NCs on the base of $GdYVO_4:Eu^{3+}$ and CeO_2 NPs provide very fast hydrophobic dye release to cells as compared to PC liposome NCs. The dye release half-lives from $GdYVO_4:Eu^{3+}$/dyes and CeO_2/dyes complexes is about 2,4 and 3 times smaller compared to that of the PC liposomes. The fast dye release is associated with the lipophilic gradient that provokes a fast transition of lipophilic dyes DiO and DiI to the abundant lipid components (cell membrane). Such membrane-mediated pathway for cellular uptake of DiI dye molecules preloaded in polymeric micelles was reported in [24]. The dye transition into the lipophilic phase causes dyes dilution in cell membranes, decrease of the aggregated dyes part and, consequently, increase of the fluorescence intensity. So, the total fluorescence intensity is sharply increased (Fig. 4a, curve *1*). In $GdYVO_4:Eu^{3+}$/dyes/cholesterol complexes, cholesterol decreases sufficiently the lipophilic gradient and noticeably slows down the dyes release process (Fig. 4b, curve *4*). The $\tau_{1/2}$ value increases more then 10 times. The lower rate of dyes release from the $GdYVO_4:Eu^{3+}$/dyes/cholesterol complexes could be also associated with another way of the complexes interaction with the cells (described above) and correlates with to the low efficiency of the total brightness increase in time observed for this system (Fig. 4a, curve *2*).

Table. Dye release constant (K) and half-life ($\tau_{1/2}$) in rat hepatocytes

Type of NCs	K, h^{-1}	$\tau_{1/2}$, h
PC Liposomes	1.5	0.46
$GdYVO_4:Eu^{3+}$	3.73	0.19
CeO_2	4.33	0.16
$GdYVO_4:Eu^{3+}$/cholesterol	0.27	2.56

4. Conclusions

The efficiency and dynamics of various NCs/dye molecules complexes accumulation in living cells and dye release kinetics have been studied using the fluorescence microspectroscopic technique and two approaches for the cell incubation with NCs/dye complexes. It has been shown that NCs on the base of $GdYVO_4:Eu^{3+}$ NPs exhibit effective accumulation in cell membranes with saturation time τ_{sat} ~ 9 h and provide the fast release of the lipophilic cargo upon the interaction with cell membranes ($\tau_{1/2}$ = 0.19 hours) that is important for certain drug administration strategies. Such high efficiency is explained by the facilitated adsorption of the complexes on cell membrane surface due to the positively charged dyes molecules, whereas the fast dyes release is due to lipophilic gradient appearance. Addition to the complexes of a lipophilic compound (cholesterol) decreases noticeable the rate of lipophilic dyes release

($\tau_{1/2}$ = 2.56 h) and reduces the affinity of NPs/dyes complex interaction with cells (τ_{sat} ~ 50 h). So, the process of NPs-to-cell interaction could be controlled. Thus, $GdYVO_4:Eu^{3+}$ NPs could be used as a nanoscale platform for intracellular delivering of hydrophobic agents that is a challenge to be solved.

References

1. O.V.Salata, *J. Nanobiotechn.*, **2**, 1 (2004).
2. M.Soloviev, *J. Nanotechnology*, **5**, 11 (2007).
3. S.Bamrungsap, Z.Zhao, T.Chen et al., *Nanomedicine*, **7**, 1253 (2012).
4. S.Parveen, R.Mishra, S.K.Sahoo, *Nanomed: Nanotech, Biol, and Med.*, **8**, 147 (2012).
5. L.Zhang, F.X.Gu, J.M.Chan et al., *Clinic. Pharmacol. & Therapeut.s*, **83**, 761 (2008).
6. Y.Liu, T-S.Niu, L.Zhang et al., *Nat. Sci.*, **2**, 41 (2010).
7. D.Peer, J.M.Karp, S.Hong et al., *Nat. Nanotechnology*, **2**, 751 (2007).
8. J.Panyam, V.Labhasetwar, *Adv. Drug Deliv. Rev.*, **55**, 329 (2003).
9. J.W.Nichols, Y.H.Bae, *Nano Today*, **7**, 606 (2012).
10. C.Bouzigues, Th.Gacoin, A.Alexandrou, *ACS Nano*, **5**, 8488 (2011).
11. A.B.Shcherbakov, N.M.Zholobak, N.Ya.Spivak et al., *Zh. Neorgan. Khimii,* **59**, 1556 (2014).
12. S.Das, J.M.Dowding, K.E.Klump et al., *Nanomedicine*, **8**, 1483 (2013).
13. V.K.Klochkov, A.V.Grigorova, O.O.Sedyh et al., *Colloids and Surfaces A: Physicochemical and Engineer Aspects*, **409**, 176 (2012).
14. E.A.Averchenko, N.S.Kavok, V.K.Klochkov et al., *J. Appl. Spectrosc.*, **81**, 754 (2014).
15. T.N.Tkacheva, S.L.Yefimova, V.K.Klochkov et al., *J. Mol. Liquids*, **199**, 244 (2014).
16. J.R.Lakowicz, Principles of Fluorescence Spectroscopy, Kluwer Academic/Plenum Publishers, New York, Boston, Dordrecht, London, Moscow (1999).
17. A.P.Demchenko, *J. Fluorescence*, **20**, 1099 (2010).
18. S.L.Yefimova, A.S.Lebed', G.Ya.Guralchuk et al., *Biopolymer and Cell*, **27**, 47 (2011).
19. S.L.Yefimova, I.Yu.Kurilchenko, T.N.Tkacheva et al., *J. Fluorescence*, **24**, 403 (2014).
20. B.Mui, L.Chow, M.J.Hope, *Meth. Enzym.*, **367**, 3 (2003).
21. S.-R.Wang, G.Renaud, J.Infante et al., *In Vitro Cell. Dev. Biol.*, **21**, 526 (1985).
22. R.P.Hauglang, Handbook of Fluorescent Probes and Research Products. Molecular Probes, New York (2002).
23. H.Chen, S.Kim, W.He et al., *Langmuir*, **24**, 5213 (2008).
24. H.Chen, S.Kim, L.Li et al., *Proc. Nat. Acad. Sci. USA*, **105**, 6596 (2008).
25. J.Lu, S.C.Owen, M.S.Shoichet, *Macromolecules*, **44**, 6002 (2011).
26. A.Mishra, R.Behera, P.K.Behera et al., *Chem. Rev.*, **100**, 1973 (2000).
27. A.Verma, F.Stellacci, *Small*, **6**, 12 (2010).
28. B.Y.Moghadam, W.-C.Hou, C.Corredor et al., *Langmuir*, **28**, 16318 (2012).
29. H.Ding, Yu.Ma, *Small*, doi: 10.1002/ smll.201401943 (2014).
30. J.L.Goldstein, R.G.W.Anderson, M.S.Brown, *Nature*, **279**, 679 (1979).
31. G.Pasa, U.S.Mishra, N.K.Tripathy et al., *J. Pharm.*, **2**, 97 (2012).